2019

Data-Driven Risk-Based Assessment of Wind-excited Tall Buildings using Surrogate Models

Laura Micheli
Iowa State University, lauramch@iastate.edu

Alice Alipour
Iowa State University, alipour@iastate.edu

Simon Laflamme
Iowa State University, laflamme@iastate.edu

Data-Driven Risk-Based Assessment of Wind-excited Tall Buildings using Surrogate Models

Abstract

The damage reported from structural and non-structural elements during severe windstorms promoted the extension of the performance-based design (PBD) philosophy to wind-excited tall buildings. A critical part of PBD is the risk assessment of the facility. Risk assessment allows the estimation of the probability of failure of the structure considering the uncertainties arising from the external hazard and the material properties. This probability is typically estimated using a nonlinear model, which permits for the evaluation of the building performance beyond the elastic regime. In wind-excited tall buildings, the use of sophisticated computational models and the long duration of typical wind events make risk-based assessment impractical and time-demanding. As a solution, this paper presents a framework for the risk-based assessment of wind-excited tall buildings using surrogate models. In the proposed framework, the surrogate models are leveraged to reduce the computational burden of time-consuming wind time history analyses. The risk of the building is quantified using the concept of fragility and hazard functions. The surrogate model is constructed using a data-driven approach, where the training data set is derived from a high-fidelity computational model. Then, the surrogate function is used as a representation of the original computational model for risk assessment and future predictions. The proposed procedure is applied to a 39-story building. The building is equipped with motion control devices for wind-induced vibrations mitigation. The wind load is simulated in the time domain as a multivariate stochastic process and numerically applied to the structure. To create the training dataset, the structural response of the building in terms of peak acceleration and inter-story drift is estimated under different wind time histories. Two cases are considered. In the first case, the mean hourly wind speed and the terrain roughness are considered as random variables, while in the second instance the capacity of the damping devices is considered as uncertain. In both cases, the surrogate model parameters are optimized using the maximum likelihood estimation method. Results show that the proposed approach can be used for improving structural resilience under extreme wind events, where the use of surrogate model represents a viable data-driven solution for uncertainty-based risk evaluation.

Disciplines

Civil Engineering | Risk Analysis | Structural Engineering

Comments

This is a manuscript of the article Micheli, Laura, Alice Alipour, and Simon Laflamme. "Data-Driven Risk-Based Assessment of Wind-excited Tall Buildings using Surrogate Models." (2019).

Data-Driven Risk-Based Assessment of Wind-excited Tall Buildings using Surrogate Models

[1] **Laura Micheli**, Ph.D. Candidate, S.M. ASCE, lauramch@iastate.edu
[2] **Alice Alipour**, Assistant Professor, M. ASCE, P.E., alipour@iastate.edu
[3] **Simon Laflamme**, Associate Professor, A.M. ASCE, laflamme@iastate.edu

Abstract

The damage reported from structural and non-structural elements during severe windstorms promoted the extension of the performance-based design (PBD) philosophy to wind-excited tall buildings. A critical part of PBD is the risk assessment of the facility. Risk assessment allows the estimation of the probability of failure of the structure considering the uncertainties arising from the external hazard and the material properties. This probability is typically estimated using a nonlinear model, which permits for the evaluation of the building performance beyond the elastic regime. In wind-excited tall buildings, the use of sophisticated computational models and the long duration of typical wind events make risk-based assessment impractical and time-demanding. As a solution, this paper presents a framework for the risk-based assessment of wind-excited tall buildings using surrogate models. In the proposed framework, the surrogate models are leveraged to reduce the computational burden of time-consuming wind time history analyses. The risk of the building is quantified using the concept of fragility and hazard functions. The surrogate model is constructed using a data-driven approach, where the training data set is derived from a high-fidelity computational model. Then, the surrogate function is used as a representation of the original computational model for risk assessment and future predictions. The proposed procedure is applied to a 39-story building. The building is equipped with motion control devices for wind-induced vibrations mitigation. The wind load is simulated in the time domain as a multivariate stochastic process and numerically applied to the structure. To create the training dataset, the structural response of the building in terms of peak acceleration and inter-story drift is estimated under different wind time histories. Two cases are considered. In the first case, the mean hourly wind speed and the terrain roughness are considered as random variables, while in the second instance the capacity of the damping devices is considered as uncertain. In both cases, the surrogate model parameters are optimized using the maximum likelihood estimation method. Results show that the proposed approach can be used for improving structural resilience under extreme wind events, where the use of surrogate model represents a viable data-driven solution for uncertainty-based risk evaluation.

1. Introduction

Performance-based engineering (PBE) is a design philosophy which enhances the resilience of structures through the integration of notions of risk and design (Federal Emergency Management Agency, 2012). Performance-based design (PBD) exploits risk-based assessment concepts to evaluate the building performance under potential hazards, considering both uncertainties inherent to external load (e.g., peak ground acceleration, mean wind speed) and properties of the structure (e.g., stiffness, damping). PBD results from a natural evolution of engineering design practice, and it is widely accepted by the seismic engineering community (Moehle and Deierlein 2004, Yang *et* *al.* 2009). Conversely, the design of civil structures for high winds currently follows prescriptive procedures, established by building codes. Literature counts several research efforts in extending PBD to wind excited structures, such as tall buildings and long span bridges (Ellingwood *et al.* 2004, Petrini and Ciampoli 2012, Seo and Caracoglia 2013, Spence and Kareem 2014). One of the major challenges in the extension of PBD to wind hazard is the large computational demand required by sophisticated computational models, especially when nonlinear relations are employed to describe the structural system (Chuang and Spence 2017). This demand, coupled with the long duration of typical wind events, makes risk-based assessment of wind excited structures time-consuming and often impractical.

Recently, the use of surrogate models or metamodels for uncertainty quantification of complex structures has gained popularity (Wang and Shan 2007, Balesdent *et al*. 2013, Downey *et al.* 2018). Metamodels, including polynomial chaos expansions, Kriging, artificial neural network, and support vector machine, are employed as a replacement of the original, often time-consuming, numerical simulation model (May and Sudret 2017, Ferrario *et al.* 2017). For example, surrogate models have been used in lieu of the original numerical models to develop seismic fragility functions (Mitropoulou and Papadrakakis 2011) and estimate seismic risk under uncertain structural and seismic parameters (Gidaris *et al.* 2015). In the wind engineering field, surrogate models have been applied to uncertainty analysis of wind turbines, considering uncertainties in environmental and operating conditions (Abdallah *et al.* 2017). Given their potential in reducing the time demand of complex computational systems, surrogate models could be ideal candidates for uncertainty analysis of wind-excited structures, and eventually integrated in a PBD approach. Nevertheless, a direct application of metamodels to wind excited tall buildings has yet to be investigated.

This paper presents a framework for risk-based assessment of wind-excited high-rise buildings using surrogate models. In the proposed framework, a radial basis function (RBF) metamodel is leveraged to reduce the computational burden of wind time history analyses. The risk of the building is quantified using fragility and hazard functions. The surrogate model is constructed using a data-driven approach, where the training and testing datasets are derived from numerical simulation models. The proposed procedure is applied to a 39-story building, located in Boston, MA. The building is equipped with passive viscous dampers for wind-induced acceleration mitigation. Two cases are investigated. In the first case, the mean hourly wind speed and the terrain roughness are considered as random variables, while in the second instance the capacity of the damping devices is assumed as uncertain.

The remainder of the paper is structured as follows. Sec. 2 describes the risk assessment approach and the metamodeling process. Sec. 3 presents the case study building and wind load characteristics. Sec. 4 discusses the results, and Sec. 5 concludes the paper.

2. Risk-Based Assessment using Surrogate Models

In this section the framework for the employment of surrogate models for risk assessment of tall buildings exposed to wind load is presented. First, a background on PBD is introduced. Next, the metamodeling process and the special case of RBF surrogate model are discussed.

2.1 PBD Background

Fig. 1 is a schematic representation of the PBD process. The variability of the external load can be represented through a site-specific hazard curve, which gives the annual probability of exceedance of the selected intensity measure (IM). In the wind PBD, a typical IM of the wind hazard is the mean hourly wind speed (Petrini and Ciampoli 2012). In order to represent uncertainties in the internal properties of the structure (e.g., stiffness, mass, damping), the structural parameters (SPs) are modeled through probability distributions. The uncertainties in external load and internal properties are propagated in the structural response through the structural analysis. Engineering demand parameters (EDP), such as inter-story drift, acceleration and velocity, are used to define the probability of failure to meet a specified performance level, conditional to the occurrence of IM (i.e., fragility curves). The fragility curves and the hazard curve can be employed to estimate the annual probability of occurrence of different damage states (DSs), which can be translated in economic losses through a loss analysis, once the damage consequences (DCs) have been established (e.g., repair, replacement costs).

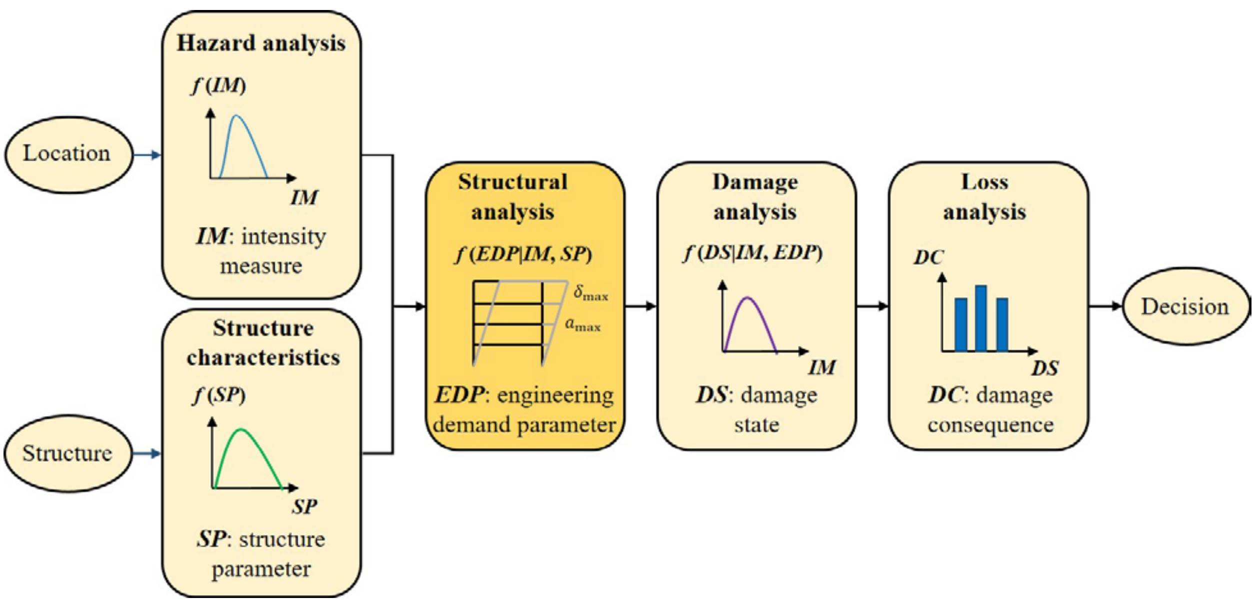

Fig. 1 Schematic representation of Performance-Based Design (PBD) procedure.

The propagation of uncertainties in the structural response requires a large number of numerical simulations to assess the structural response under a variety of scenarios. Metamodels can be employed as substitute of the original, often computationally expensive, numerical simulation model to perform the structural analysis (as highlighted in Fig. 1). Specifically, the metamodeling process consists of constructing a simplified mathematical representation that emulates the response of the system based on available input/output data. In the PBD framework, the inputs could be the uncertainties in the SPs and IM, while the output may be expressed in terms of a single or multiple EDPs. The constructed surrogate can be used to predict outputs in correspondence of new inputs, and generate fragility curves without the necessity of performing structural analysis.

2.2 Metamodeling Process

The objective of the metamodeling process is to map the unknown relation between inputs and outputs of a system. The fundamental steps necessary to build a surrogate are as follows:

Step 1: Identify the input variables vector $\mathbf{x} = \{x_1, x_2, \ldots, x_k\}^{\mathrm{T}}$ and its range of variability.

Step 2: Sampling N values of $\mathbf{x}$ from the space domain and create a set of N observations $S = \{(\mathbf{x}^{(i)}, y_i), i = 1,\ldots N\}$, where the output y_i derives from the original numerical simulation model.

Step 3: Divide the observation set in two subsets: the training (size n) and the testing subsets (size n_t).

Step 4: Learn the underlying mapping $y = f(\mathbf{x})$ that converts the vector $\mathbf{x}$ into a scalar y, exploiting the training data set (i.e., supervised learning).

Step 5: Evaluate the surrogate model accuracy using the testing data set.

The learning algorithms used in Step 4 depend on the type of metamodel selected. In this paper, a RBF-based model is used. The output y can be expressed as (Forrester and Keane 2008):

$$\mathbf{y} = \mathbf{w}^{\mathrm{T}}\boldsymbol{\Psi} \tag{1}$$

where $\mathbf{w}$ is a vector of weights, and $\boldsymbol{\Psi} \in \mathbb{R}^{n\times n}$ is the basis functions matrix, which elements are defined as:

$$\boldsymbol{\Psi}_{i,j} = \psi\left(\left\|\mathbf{x}^{(i)} - \mathbf{x}^{(j)}\right\|\right) \tag{2}$$

where $\left\|\mathbf{x}^{(i)} - \mathbf{x}^{(j)}\right\|$, for i, j = 1, …, n, represents the Euclidean distance between two generic samples in the training set, assuming that the centers of the basis functions coincide with the data points, and ψ is the radial basis function. In this study, a Gaussian radial basis function is selected:

$$\psi\left(\left\|\mathbf{x}^{(i)} - \mathbf{x}^{(j)}\right\|\right) = \exp\left(-\frac{1}{2\sigma^2}\left\|\mathbf{x}^{(i)} - \mathbf{x}^{(j)}\right\|^2\right) \tag{3}$$

where σ is the width of the Gaussian function. It follows that the model parameters to calibrate are $\mathbf{w}$ and σ.

In order to estimate the width of the Gaussian function, σ, the cross-validation error is minimized (Forrester and Keane 2008). The cross-validation error is computed using the *leave-one-out* procedure, which consists dividing the training set into m subsets containing approximately the same number of samples q, randomly selected. Then, one of the m subset is excluded from the computation in turn and the model is fitted to the remaining (m – 1) subsets. At each iteration the error is calculated exploiting the excluded subset as testing set, and expressed as:

$$E_{\mathrm{cv}} = \frac{1}{q}\sum_{i=1}^{q}(y_i - \hat{y}_i) \tag{4}$$

where $\hat{y}_i$ is the estimate of y, obtained with Eq. (1), and y_i is the actual output value. The total cross-validation error is the sum of the m values of E_{cv}.

Once σ has been identified, it can be replaced in Eq. (3), and the weights can be estimated inverting Eq. (1):

$$\mathbf{w} = \boldsymbol{\Psi}^{-1}\mathbf{y} \tag{5}$$

After all the parameters have been estimated, Eq. (1) can be directly used for the prediction of new outputs, given new input vectors $\mathbf{x}$.

3. Case Study

This section presents the case study building, along with the numerical technique used to simulate its response. The structure is equipped with passive viscous dampers for wind-induced vibration mitigation. Next, the wind load and the uncertainty cases under examination are described.

3.1 High-rise Building

The metamodeling process is applied to a 39-story office tower, located in Boston, MA. The building height is 163 m and the lateral resisting system is a moment-frame tube system. The inter-story height is equal to 7.4 m at the ground and roof levels, and 3.9 m at all the other floors. The weak direction of the building is numerically simulated as a spring-dashpot-mass system. In this direction the building is equipped with 15 sets of two viscous dampers, installed at every other floor, starting from the 5$^{\text{th}}$ floor up to the 33$^{\text{th}}$ (McNamara and Taylor 2003).

The state-space formulation is employed to simulate the building response. The equation of motion for the 39-story building can be expressed as (Connor and Laflamme 2014):

$$\mathbf{M\ddot{u}} + \mathbf{C\dot{u}} + \mathbf{Ku} = \mathbf{E}_w\mathbf{W} - \mathbf{E}_f\mathbf{F} \tag{6}$$

where $\mathbf{u} \in \mathbb{R}^{39\times1}$, $\dot{\mathbf{u}} \in \mathbb{R}^{39\times1}$, $\ddot{\mathbf{u}} \in \mathbb{R}^{39\times1}$ are displacement, velocity, and acceleration vectors, respectively, $\mathbf{M} \in \mathbb{R}^{39\times39}$, $\mathbf{C} \in \mathbb{R}^{39\times39}$, and $\mathbf{K} \in \mathbb{R}^{39\times39}$ represent mass, damping, and stiffness matrices, respectively, $\mathbf{W} \in \mathbb{R}^{39\times1}$ is the wind load vector, $\mathbf{F} \in \mathbb{R}^{15\times1}$ is the damping force vector, $\mathbf{E}_w \in \mathbb{R}^{39\times39}$ and $\mathbf{E}_f \in \mathbb{R}^{39\times15}$ are the load and the damping force location matrices. The state space formulation of this equation is:

$$\dot{\mathbf{U}} = \mathbf{AU} + \mathbf{B}_w\mathbf{W} - \mathbf{B}_f\mathbf{F} \tag{7}$$

where $\mathbf{U} = [\mathbf{u} \quad \dot{\mathbf{u}}]^{\mathrm{T}} \in \mathbb{R}^{78\times1}$ is the state vector with:

$$\mathbf{A} = \begin{bmatrix} \mathbf{0} & \mathbf{I} \\ -\mathbf{M}^{-1}\mathbf{K} & -\mathbf{M}^{-1}\mathbf{C} \end{bmatrix}_{78\times78} \tag{8}$$

$$\mathbf{B}_f = \begin{bmatrix} \mathbf{0} \\ \mathbf{M}^{-1}\mathbf{E}_f \end{bmatrix}_{78\times15} \tag{9}$$

$$\mathbf{B}_w = \begin{bmatrix} \mathbf{0} \\ \mathbf{M}^{-1}\mathbf{E}_w \end{bmatrix}_{78\times39} \tag{10}$$

The discrete form of the Duhamel integral is used to solve Eq. (7) (Connor and Laflamme 2014):

$$\mathbf{U}(t+\Delta_t) = \exp(\mathbf{A}\Delta_t)\,\mathbf{U}(t) + \mathbf{A}^{-1}[\exp(\mathbf{A}\Delta_t) - \mathbf{I}]\left[\mathbf{B}_w\mathbf{W}(t) - \mathbf{B}_f\mathbf{F}(t)\right] \tag{11}$$

where Δ_t is the time interval (taken as 0.01 s) and $\mathbf{I} \in \mathbb{R}^{39\times39}$ is the identity matrix. The dynamic characteristics of the building, such as **M**, **C**, and **K** matrices, are reported in Cao *et al.* (2016).

The damping force exerted by a viscous damper can be written as (Connor and Laflamme 2014):

$$F_v = c \cdot \mathrm{sgn}(\dot{u}) \tag{12}$$

where c represents the damping coefficient, $\dot{u}$ is the relative velocity, and $\mathrm{sgn}(\dot{u})$ indicates the sign of $\dot{u}$. The damping coefficients are taken as 52,550 kN·s/m for the dampers below the 26th floor, and 35,000 kN·s/m for the devices above the 26th floor (McNamara *et al.* 2003). The damper nominal capacity, $F_{v,\max}$, is equal to 1,350 kN for the dampers below the 26th floor, and 900 kN for the devices above the 26th floor (Laflamme *et al*. 2012).

3.2 Wind load

The wind load vector **W** in Eq. (7) is taken as the along-wind fluctuating forces acting on the building in the simulated direction. At the j-th floor W_j can be expressed as (Simiu and Scalan 1996):

$$W_j = \rho\, c_D\, A_j\left(V_{m,j} + V_{t,j}\right) \tag{13}$$

where ρ is the air density (taken as 1.25 kg/m^3), c_D is the drag coefficient (equal to 1.5), A_j is the projected area of the building normal to the wind flow at the j-th level, $V_{m,j}$ is the mean wind speed at the j-th floor, and $V_{t,j}$ is the fluctuating wind velocity generated by the wind turbulence. The mean wind speed at the j-th floor can be written as (Simiu and Scanlan 1996):

$$V_{m,j} = V_{m,10}\frac{\ln(z/z_0)}{\ln(10/z_0)} \tag{14}$$

where $V_{m,10}$ is the mean wind speed at a reference height z = 10 m above the ground, z denotes the height of the generic floor, and z_0 is the terrain roughness (nominal value equal to 0.03 m for sub-urban terrain). The fluctuating wind speed is simulated using the spectral approach outlined by Shinozuka and Deodatis (1991) and Deodatis (1996). Fig. 2 shows an example of wind force time history at the last floor of the structure, along with the building response in terms of acceleration.

3.3 Analyzed Cases

In this study, the peak acceleration experienced by the building is taken as output of the system:

$$y = \max|\ddot{\mathbf{u}}(t)| \tag{15}$$

The peak acceleration is selected as output because it represents the design variable for the viscous dampers, which were installed in the building to reduce the high acceleration levels experienced by the structure under wind load (McNamara *et al.* 2003).

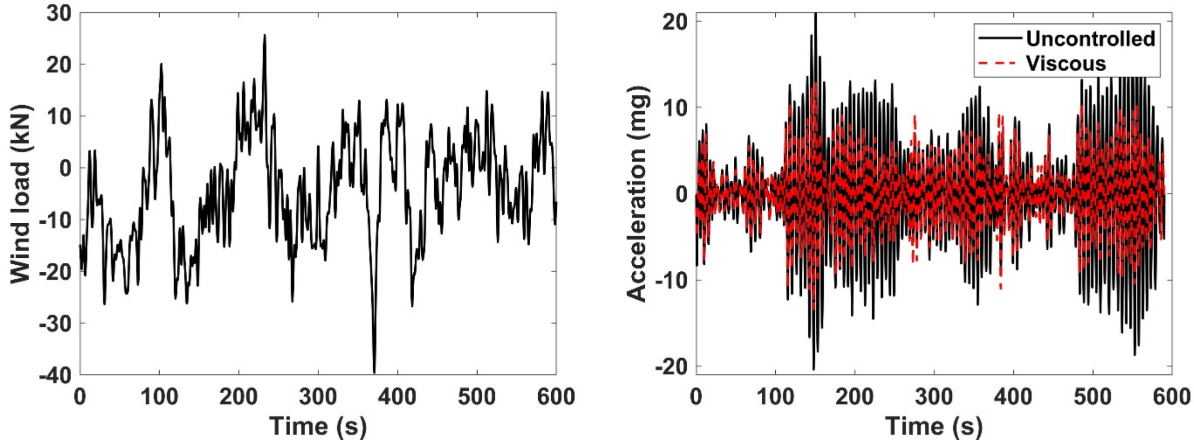

(a) (b)

Fig. 2 (a) Wind load time series at the 39th floor with wind load parameters $V_{m,10}$ = 21 m/s and $z_0 = 0.03$ m; and (b) corresponding acceleration response for building without damping devices (Uncontrolled) and with viscous dampers (Viscous).

Two uncertain cases are investigated. In the first case, the mean wind speed at a reference height z = 10 m, $V_{m,10}$ (Eq. 14), and the terrain roughness, z_0 (Eq. 14), are considered as uncertain. It follows that the input vector in case 1 is $\mathbf{x} = [V_m \ z_0]^{\mathrm{T}}$. In case 2, the wind load and capacity of the dampers are considered as variables. In this case, the input vector is $\mathbf{x} = [V_m \ z_0 \ F_{v,\max,1} \ F_{v,\max,2} \ldots F_{v,\max,15}]^{\mathrm{T}}$, resulting from the two wind load variables and the 15 dampers capacities.

The range of variability of the input variables is reported in Table 1. The wind speed $V_{m,10}$ is varied between 5 and 28 m/s, representing minimum and maximum wind speeds that the structure will likely experience during its lifespan (Micheli *et al.* 2017). The terrain roughness range is selected as 0.01 and 0.03 m following recommendations by Chuang and Spence (2017). In case 2, it is assumed that the maximum capacity of the single viscous damper can vary between 50% and 100% of $F_{v,\max}$. This assumption is a representation of wear and time effects, such as fatigue and materials degradation, which could cause a decrement in the nominal damping capacity of the single device.

Table 1: Inputs variables

Case	**Variables**	**Symbol**	**Range of variability**	***k***
1	Mean wind speed	$V_{m,10}$	5 – 28 m/s	2
	Terrain roughness	z_0	0.01 – 0.03 m	
2	Mean wind speed	$V_{m,10}$	5 – 28 m/s	17
	Terrain roughness	z_0	0.01 – 0.03 m	
	Dampers capacity below 26th	$F_{v,\max}$	675 – 1,350 kN	
	Dampers capacity above 26th	$F_{v,\max}$	450 – 900 kN	

The space filling Latin hypercube method is employed to sample a total of N = 750 different **x** vectors for each variable in Table 1. For each **x**, the output y (Eq. (15)) is obtained simulating the system through Eq. (7) - (11). When the matrix in Eq. (2) is poorly conditioned, $\mathbf{\Psi}$ is replaced with its nearest symmetric positive matrix (Higham 1988).

The investigation is conducted considering the building equipped with passive viscous dampers and without dampers (i.e., uncontrolled structure). As an example, Fig. 3 plots the maximum acceleration experienced by the uncontrolled building and structure equipped with viscous dampers, with and without uncertainties in the damping capacity, for two different wind speeds. One can observe that when the viscous dampers capacity is varied (case 2), the response is slightly higher in comparison with the dampers set at their nominal capacities (case 1).

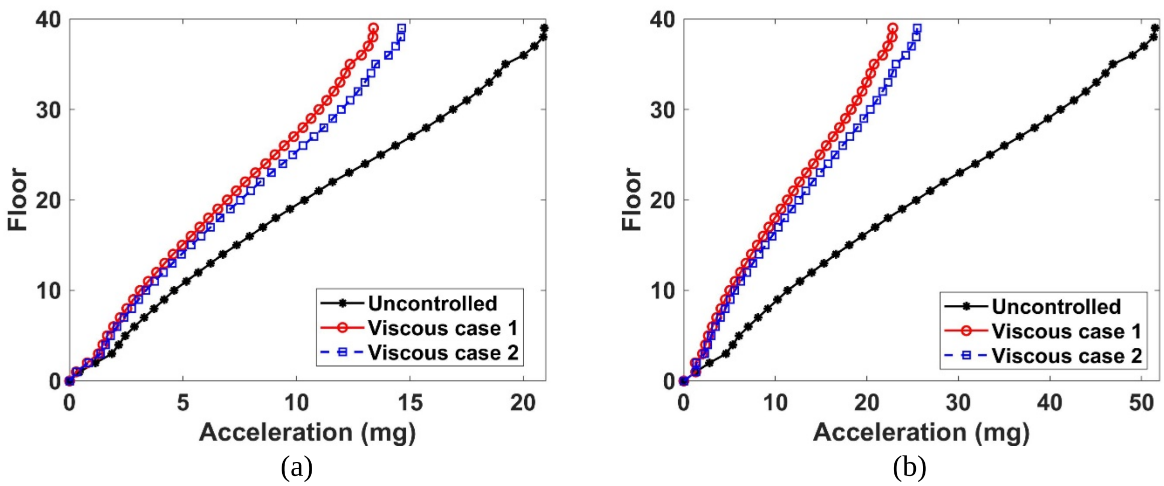

Fig. 3 Maximum acceleration profile for uncontrolled building and building equipped with viscous dampers, under wind load with parameters $z_0 = 0.03$ m and: (a) $V_{m,10}$ = 21 m/s; (b) $V_{m,10}$ = 28 m/s.

4. Metamodel Accuracy

In order to identify an optimal data set size, a parametric study is conducted. The study starts with the selection of n = 200 observations for the training set, and $n_t = 0.25 \times n = 50$ for the testing set (Forrester and Keane 2008). In order to determine the metamodel accuracy, the following two error metrics are defined:

$$\mathrm{RMSE} = \sqrt{\frac{\sum_{i=1}^{n_t}(y_i - \hat{y}_i)^2}{n_t}} \tag{16}$$

$$\mathrm{NMAE} = \frac{\max_{n_t}|y_i - \hat{y}_i|}{n_t\,\sigma_y} \tag{17}$$

where RMSE is the root mean square error, NMAE represents the normalized maximum absolute error, $\hat{y}_i$ denotes the peak acceleration estimated with the RBF metamodel (Eq. (1)), y_i is the true value of the peak acceleration (calculated with the numerical simulation model), and σ_y is the standard deviation of the testing data set (true values). The errors are evaluated on the testing data set after the metamodel is calibrated with the training data set.

Table 2 reports the errors for cases 1 and 2. The RMSE is normalized and expressed in percentage, in order to conduct a fair comparison between different cases. At each step of the parametric study, the number of samples is increased by 200 observations, until the RMSE falls within the 5% threshold. Results in Table 2 demonstrate that the RMSE is approximately equal to 5% in all the cases, independent of the training set size. Also the NMAE is low in all the cases, indicating a good local fit of the data. The following analyses are performed using the RBF model trained with *n* = 600 samples, since it led to slightly more accurate results for the case 2-viscous dampers.

Table 2: Errors as function of the uncertainty case and number of samples

Case	**Control Strategy**	**Training n**	**Testing n_t**	**RMSE (%)**	**NMAE (%)**
Case 1	Viscous	200	50	4.30 %	1.05
		400	100	4.29 %	0.66
		600	150	4.11 %	0.25
	Uncontrolled	200	50	4.48 %	1.00
		400	100	4.58 %	0.57
		600	150	4.56 %	0.25
Case 2	Viscous	200	50	6.72 %	1.44
		400	100	6.35 %	0.82
		600	150	5.07 %	0.45

5. Risk Assessment with RBF

This section presents the application of the RBF metamodel for risk assessment of the 39-story building. The objective is the derivation of fragility functions, which express the probability of exceedance of the structure of a pre-selected limit state, conditional to the occurrence of a certain wind speed. Fragility curves are traditionally obtained through Monte Carlo analysis, performing a large number of time consuming simulations. In this study, the RBF model trained in the previous sections is employed as substitute of the original computational model.

The mean wind speed, $V_{m,10}$, is considered as the intensity measure, and the variables reported in Table 1 as uncertain parameters. These variables are modeled with the uniform distributions listed in Table 1, except for the mean wind speed. A Weibull distribution with scale parameter of 14.9 and shape parameter of 6.4 is assumed for $V_{m,10}$ (Micheli *et al.* 2017). The Latin hypercube sampling method is employed to generate M = 5,000 sample from these distributions. As an example, only one limit state (LS) is considered. It is assumed that LS is exceeded when the peak acceleration experienced by the building is y > 25 mg (Micheli *et al.* 2018). It follows that the probability of exceedance of the LS, given the occurrence of $V_{m,10}$, can be estimated as:

$$P(V_{m,10}) = \frac{\sum_{i=1}^{M} L_i}{M} \tag{18}$$

where L_i is an index, equal to 1 if y_i > 25 mg, equal to zero otherwise. The fragility curve is obtained fitting the P values at different $V_{m,10}$ with the maximum likelihood method, assuming a lognormal distribution function. Fig. 4 (a) – (c) plot the fragility curves of the 39-story building obtained with the RBF metamodel predictions. The fragility functions obtained with the numerical simulation algorithms are also illustrated, and taken as benchmark.

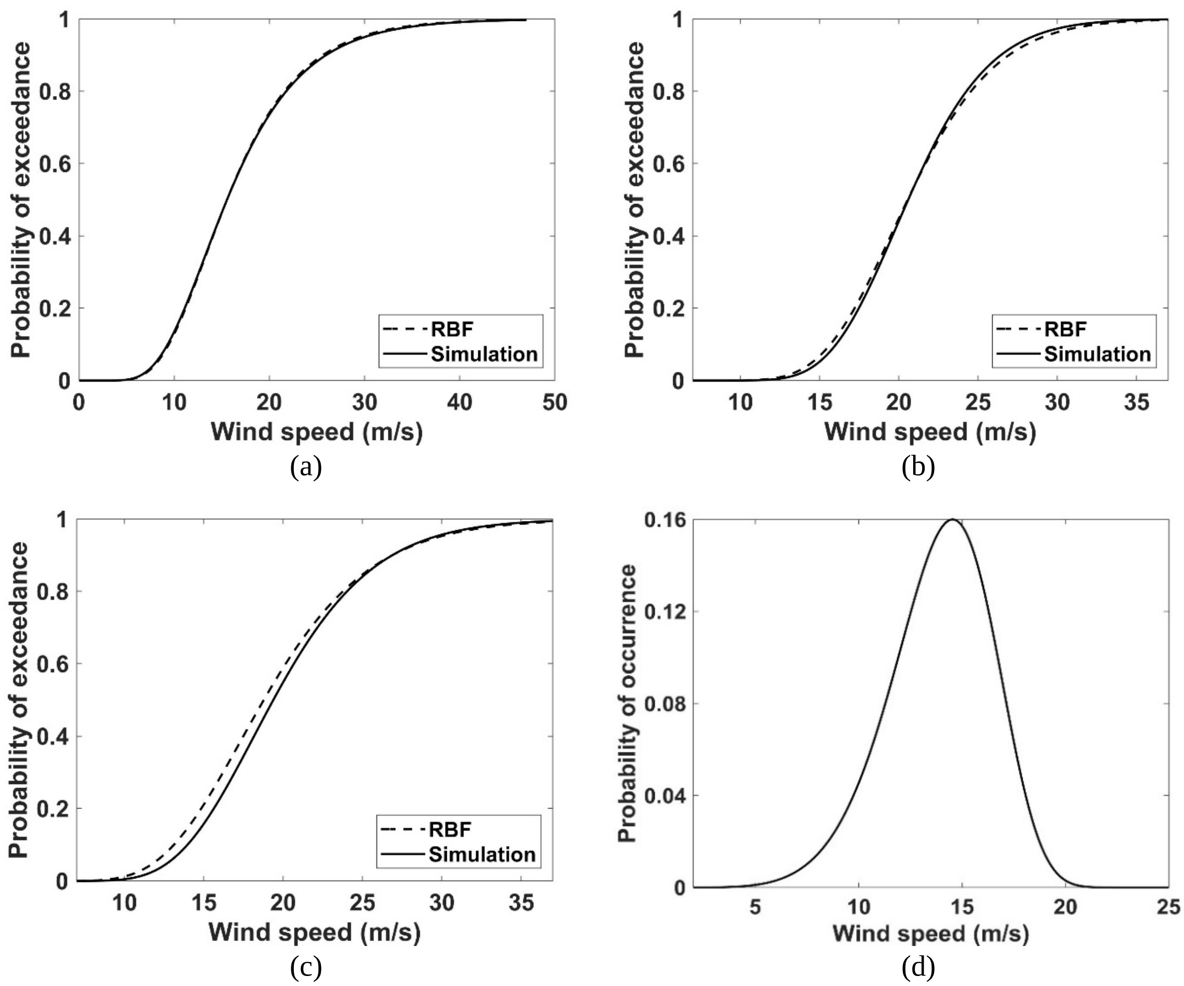

Fig. 4 Fragility curves for the 39-story building for: (a) uncontrolled building, case 1; (b) building with viscous dampers, case 1; (c) building with viscous dampers, case 2; (d) annual wind speed hazard curve for Boston (MA).

Results in Fig. 4 (a) – (c) show a good agreement between actual and predicted fragility curves in case 1, for both building with and without viscous dampers. In case 2, the RBF model tends to overestimate the probability of exceedance of LS in the low wind speed region. This loss of accuracy could be attributed to the larger space dimension of case 2, which involves k = 17 random variables (in comparison with case 1, where k = 2). A cross-comparison between the control strategies demonstrates that the probability of failure is higher for the uncontrolled building, as expected. Additionally, in the case with viscous dampers, one can notice that the probability of exceedance in case 2 is larger than in case 1, due to the added uncertainties in the damping capacity.

The fragility functions developed with RBF and original simulation models are used in combination with the wind hazard curve to obtain the annual probability of exceedance of LS, conditional to the wind speed $V_{m,10}$. The hazard curve, shown in Fig. 4 (d), was derived from meteorological data collected in a previous investigation by the authors (Micheli *et al.* 2017). Fig. 5 reports the annual probability of exceedance curves, as function of the analyzed cases. The figure demonstrates that, in the uncontrolled case, predicted and simulated curves match. In the viscous damper cases, a substantial difference between the predicted and the true functions can be observed, especially for Viscous – case 2. This is the result of the slight overestimation of the corresponding fragility curve in Fig. 4 (c).

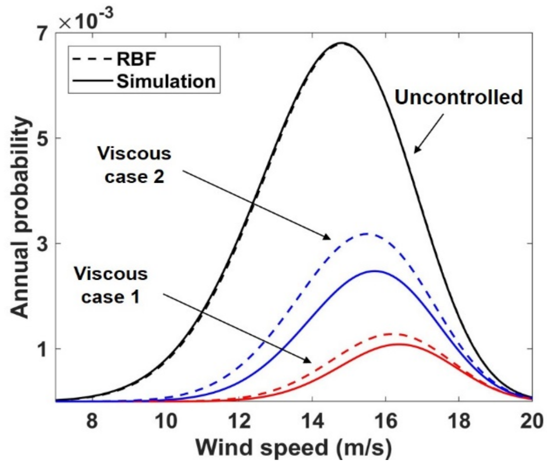

Fig. 5 Annual probability of exceedance of LS for the investigated cases.

6. Conclusions

In this paper, an investigation on the use of a radial basis function (RBF) metamodel for risk-based assessment of wind-excited tall buildings equipped with damping devices was presented. The structural risk was expressed in terms of annual probability of exceedance of a selected limit state, and quantified using fragility and hazard functions. The fragility functions were obtained exploiting the prediction capability of the RBF, which was constructed using a data-driven approach where the training and testing datasets were derived from numerical simulation models.

To evaluate the effectiveness of the framework a 39-story building, located in Boston (MA), was employed as a case study. The building was equipped with passive viscous dampers, and subjected to synthetic wind time series. Two uncertainty cases were investigated, concerning uncertainties in wind load, and maximum damping capacity of the devices, respectively. The metamodels were trained to estimate the peak acceleration experienced by the structure as function of the inputs (i.e., wind load, dampers characteristics). A parametric study was conducted to evaluate the optimal sizes of training and testing data sets, and the accuracy of the metamodel was estimated. Lastly, the RBF model was used to build fragility functions for the 39-story building, with and without viscous dampers. In the majority of the cases, the fragility functions predicted with the RBF resulted in a good agreement with the actual curves, obtained using the original numerical model. In the viscous dampers case, a slight difference between the predicted and the true fragility function can be observed, due to the larger space representation. A larger training data set may be a solution for obtaining more accurate results. The main advantage of using RBF surrogate in the derivation of the fragility curves is given by the relevant savings in computational time. Additionally, results of the risk-assessment analysis highlighted the importance of considering uncertainties in the dampers performance evaluation.

This investigation demonstrated the feasibility of applying metamodels for risk analysis of tall buildings equipped with damping devices. Future work will include the comparison of different types of metamodels and their integration in a PBD approach.

Acknowledgement

This paper is based upon work supported by the National Science Foundation under Grant No. 1537626. Their support is gratefully acknowledged. Any opinions, findings, and conclusions or recommendations expressed in this material are those of the authors and do not necessarily reflect the views of the National Science Foundation.

References

Abdallah, I., Lataniotis, C., & Sudret, B. (2017). Hierarchical Kriging for multi-fidelity aero-servo-elastic simulators-Application to extreme loads on wind turbines. *arXiv preprint arXiv:1709.07637*.

Balesdent, M., Morio, J., & Marzat, J. (2013). Kriging-based adaptive importance sampling algorithms for rare event estimation. *Structural Safety*.

Cao, L., Laflamme, S., Taylor, D., & Ricles, J. (2016). Simulations of a variable friction device for multihazard mitigation. *Journal of Structural Engineering*.

Chuang, W. C., & Spence, S. M. (2017). A performance-based design framework for the integrated collapse and non-collapse assessment of wind excited buildings. *Engineering Structures*.

Connor, J., & Laflamme, S. (2014). *Structural motion engineering.* Springer.

Deodatis, G. (1996). Simulation of ergodic multivariate stochastic processes. *Journal of engineering mechanics*, 778-787.

Downey, A., Sadoughi, M., Laflamme, S., & Hu, C. (2018). Incipient Damage Detection for Large Area. *IEEE Journal*.

Ellingwood, B. R., Rosowsky, D. V., Li, Y., & Kim, J. H. . (2004). Fragility assessment of light-frame wood construction subjected to wind and earthquake hazards. *Journal of Structural Engineering*, 1921-1930.

Federal Emergency Management Agency (FEMA). (2012). *Seismic performance assessment of buildings, Volume 1 - Methodology*. Washington, DC: FEMA Pubblication P-58-1.

Ferrario, E., Pedroni, N., Zio, E., & Lopez-Caballero, F. . (2017). Bootstrapped Artificial Neural Networks for the seismic analysis of structural systems. . *Structural Safety*.

Forrester, A., & Keane, A. (2008). *Engineering design via surrogate modelling: a practical guide.* Engineering design via surrogate modelling: a practical guide.

Gidaris, I., Taflanidis, A. A., & Mavroeidis, G. P. (2015). Kriging metamodeling in seismic risk assessment based on stochastic ground motion models. *Earthquake Engineering & Structural Dynamics*.

Higham, N.J. (1988). Computing a nearest symmetric positive semidefinite matrix. *Linear algebra and its applications*.

Laflamme, S., Taylor, D., Abdellaoui Maane, M., & Connor, J. J. . (2012). Modified friction device for control of large-scale systems. *Structural control and health monitoring*, 548-564.

Mai, C. V., & Sudret, B. . (2017). Surrogate models for oscillatory systems using sparse polynomial chaos expansions and stochastic time warping. *SIAM/ASA Journal on Uncertainty Quantification*.

Mcnamara, R. J., & Taylor, D. P. (2003). Fluid viscous dampers for high-rise buildings. . *The structural design of tall and special buildings*, 145-154.

Micheli, L., Alipour A., Laflamme S. (2018). Performance-based design for wind-excited tall buildings equipped with high performance control systems. *Structures Congress 2018*.

Micheli, L., Cao, L., Gong, Y., Cancelli, A., Laflamme, S., & Alipour, A. (2017). Probabilistic performance-based design for high performance control systems. *Active and Passive Smart Structures and Integrated Systems 2017* .

Mitropoulou, C. C., & Papadrakakis, M. (2011). Developing fragility curves based on neural network IDA predictions. *Engineering Structures*.

Moehle, J., & Deierlein, G. G. (2004). A framework methodology for performance-based earthquake engineering. *13th world conference on earthquake engineering* .

Petrini, F., & Ciampoli, M. (2012). Performance-based wind design of tall buildings. *Structure and Infrastructure Engineering*.

Seo, D. W., & Caracoglia, L. . (2013). Estimating life-cycle monetary losses due to wind hazards: Fragility analysis of long-span bridges. *Engineering Structures*.

Shinozuka, M., & Deodatis, G. . (1991). Simulation of stochastic processes by spectral representation. . *Applied Mechanics Reviews*, 191-204.

Simiu, E., & Scanlan, R. H. (1996). *Wind effects on structures.* Wiley.

Spence, S. M., & Kareem, A. (2014). Performance-based design and optimization of uncertain wind-excited dynamic building systems. *Engineering Structures*.

Wang, G. G., & Shan, S. . (2007). Review of metamodeling techniques in support of engineering design optimization. *Journal of Mechanical design*.

Yang, T. Y., Moehle, J., Stojadinovic, B., & Der Kiureghian, A. (2009). Seismic performance evaluation of facilities: methodology and implementation. *Journal of Structural Engineering*.